CHAPTER – 3

ROBUST NONLINEAR EXCITATION CONTROL STRATEGY

3.1 Introduction:

Improving the transient stability of power systems is one of the major issues in power system control. It is well known that control through the excitation loop of synchronous generators is one of the most cost effective ways to stabilize power system [46]. Unfortunately, power systems are large scale nonlinear system; the characteristics of conventional controllers that are designed based on approximately linearized power system models, such as power system stabilizers, vary significantly with respect to the changes in operating conditions. The use of advanced control techniques in power systems has been one of the more promising application areas. To enhance the transient stability of power systems, in recent years a great deal of attention has been paid to the application of nonlinear control techniques, particularly feedback linearization approaches [30-32] where nonlinear feedback is used to cancel the inherent system nonlinearities. By using feedback linearization technique, a nonlinear power system model can be directly transformed to a system whose closed-loop dynamics are linear over the whole or a wide operating region and thus linear control theories can be applied to this feedback linearized model to design an effective control law. Most of the nonlinear excitation controllers [38-45] are designed based on the feedback linearization technique. In majority of these applications, a particular variety of this method called direct feedback linearization (DFL) has been used [39-45]. DFL allows more feasibility to preserve physical states than the original geometric algorithm version [30-32]. One of the problem that challenges the feedback linearization method is that the parameters of the system must be accurately known for exact cancellation of the system nonlinearities. Power systems are uncertain, complex multivariable dynamic systems. Due to variety of effects the configuration of a power system is not constant. Thus important parameters, such as effective line reactances, in a power system always have some uncertainties. Such parametric uncertainties challenge the robustness of the feedback linearizing controllers. Robustness issues for the DFL excitation controllers have been addressed by researchers [41-45] who used robust control techniques for linear systems [33-35] together with DFL design technique to design robust nonlinear excitation controller for power systems. These approaches are theoretically elegant no doubt, but in a practical power system,

determination of the proper bounds for the uncertainties is not a trivial task considering the wide range of operating conditions and wide variety of disturbances a power system may be subjected to. In the present work, a simple strategy for nonlinear robust excitation control has been proposed which utilities DFL technique for taking into account the nonlinearities of the power system model, but no additional considerations are required for the control robustness; robustness comes naturally due to the selection of the linearizing feedback signals. In this chapter, a single-machine infinite bus (SMIB) power system has been considered for simulation studies to demonstrate the effectiveness of the proposed control strategy. Since an SMIB system qualitatively exhibits important aspects of the behaviour of a real power system and is relatively simple to study, such a simplified system is extremely useful in describing the general concepts of power system stability, the influence of various factors upon stability, and alternative controller concepts.

3.2 Power System Model:

The actual dynamic response of a synchronous generator in the practical power system is very complex, and is very difficult to deal with in the controller design unless some simplifications [46-47] are made. It has been shown that when designing the excitation controller, the classical third-order dynamic model of generator can be used [46]. Let us consider the SMIB power system shown in Fig.3.1. It consists of a single generator connected through two parallel transmission lines to a very large network approximated by an infinite bus. The classical third-order model of the SMIB system can be written as follows [39]:

Mechanical Equations:

$$\dot{\delta}(t) = \omega(t) - \omega_o \tag{3.1}$$

$$\dot{\omega}(t) = -\frac{D}{2H}(\omega(t) - \omega_o) + \frac{\omega_o}{2H}(P_m - P_e(t)) \tag{3.2}$$

Note: (t) will be used to indicate function of time throughout this test.

Generator Electrical Dynamics:

$$\dot{E}'_q(t) = \frac{1}{T'_{do}}\left(E_f(t) - E_q(t)\right) \tag{3.3}$$

Electrical Equations:

$$E_q(t) = \frac{x_{ds}}{x'_{ds}}E'_q(t) - \frac{x_d - x'_d}{x'_{ds}}V_S\cos\delta(t) \tag{3.4}$$

$$P_e(t) = \frac{V_S E_q(t)}{x_{ds}}\sin\delta(t) \tag{3.5}$$

$$I_q(t) = \frac{V_S}{x_{ds}}\sin\delta(t) = \frac{P_e(t)}{x_{ad}I_f(t)} \tag{3.6}$$

$$\mathrm{Q_e}(t) = \frac{V_S}{x_{ds}}E_q(t)\cos\delta(t) - \frac{V_S^2}{x_{ds}} \tag{3.7}$$

$$E_q(t) = x_{ad}I_f(t) \tag{3.8}$$

$$E_f(t) = k_e u_f(f) \tag{3.9}$$

where

$\delta(t)$	power angle of the generator (in rdian);
$\omega(t)$	angular speed of the generator (in rad/s);
P_m	mechanical input power (in p.u.);
$P_e(t)$	active power delivered by the generator (in p.u.);
$Q_e(t)$	reactive power delivered by the generator (in p.u.
$E_q(t)$	quadrature axis EMF (in p.u.);
$E'_q(t)$	quadrature axis transient EMF (in p.u.);
$I_q(t)$	quadrature axis current of the generator (in p.u.);
$E_f(t)$	the equivalent EMF in the excitation coil (in p.u.);

$u_f(t)$ input to the SCR amplifier of the excitation system (in p.u.);

$I_f(t)$ excitation current;

$V_t(t)$ terminal voltage of the generator (in p.u.);

V_s infinite bus voltage (in p.u.) – reference ;

D damping constant (in p.u.);

H inertia constant (in secs);

T'_{do} direct axis transient open circuit time constant (in secs) ;

x_d direct axis reactance (in p.u.);

x'_d direct axis transient reactance (in p.u.);

ω_o synchronous speed (in rad/secs);

k_e gain of the excitation amplifier;

x_{ad} mutual reactance between the excitation cil and the stator coil (in p.u.);

x_{ds} = $x_d + x_T + ½\ x_L$;

x'_{ds} = $x'_d + x_T + ½\ x_L$;

3.3 Existing DFL Excitation Control Strategies:

Most of the DFL nonlinear excitation control strategies proposed earlier [39-45] are based on the DFL formulation suggested by Y. Wang et.al [39]. Applying the DFL transformation proposed there the nonlinear power system model given by equations (3.1 – 3.9) is transformed into the following linearized model:

$$\Delta\dot{\delta}(t) = \Delta\omega(t) \qquad (3.10)$$

$$\Delta\dot{\omega}(t) = -\frac{D}{2H}\Delta\omega(t) - \frac{\omega_o}{2H}\Delta P_e(t) \qquad (3.11)$$

$$\Delta\dot{P}_e(t) = -\frac{1}{T'_d}\Delta P_e(t) + \frac{1}{T'_d}v_f(t) \qquad (3.12)$$

Where $v_f(t)$ is the new input called pseudo control and given by

$$v_f(t) = \frac{V_S}{x_{ds}} \sin\delta(t) \left[k_e u_f(t) + T'_{do}(x_d - x'_d) \frac{V_S}{x_{ds}} \sin\delta(t)\Delta\omega(t) \right] + T'_d \frac{V_S}{x_{ds}} E_q(t) \cos\delta(t)\Delta\omega(t) - P_m \quad (3.13)$$

where $T'_d = \frac{x'_{ds}}{x_{ds}} T'_{do}$

$\Delta\delta(t) = \delta(t) - \delta_o$; δ_o is the equilibrium value of $\delta(t)$

$\Delta\omega(t) = \omega(t) - \omega_o$;

$\Delta P_e(t) = P_e(t) - P_m$; P_m is assumed to remain constant at its pre-fault value.

The linearizing control law is then given by

$$u_f(t) = \frac{x_{ds}}{k_e V_S \sin\delta(t)} \left[v_f(t) - T'_d \frac{V_S}{x_{ds}} E_q(t) \cos\delta(t)\Delta\omega(t) + P_m \right] - T'_{do}(x_d - x'_d) \frac{V_S}{x_{ds}} \sin\delta(t)\Delta\omega(t) \quad (3.14)$$

The transformation (3.14) is obviously invertible except when $\sin\delta(t) = k \times 180^o$ (k is any integer) which is not in the normal working region.

Since $\delta(t)$ is difficult to measure, from the point of view of practical realizability, equation (3.14) is expressed in the following form using equations (3.6) and (3.7):

$$v_f(t) = I_q(t) \left[k_e u_f(t) + T'_{do}(x_d - x'_d) I_q(t)\Delta\omega(t) \right] + T'_d \left[Q_e(t) + \frac{V_S^2}{x_{ds}} \right] \Delta\omega(t) - P_m \quad (3.15)$$

Corresponding linearizing control law is given by

$$u_f(t) = \frac{1}{k_e I_q(t)}\left[v_f(t) - T'_d\left\{ Q_e(t) + \frac{V_S^2}{x_{ds}} \right\}\Delta\omega(t) - (x_d - x'_d)T'_{do}\Delta\omega(t)I_q^2(t) + P_m \right] \tag{3.16}$$

Inversion is possible except when $I_q(t) = 0$ (corresponding to the situation $\delta(t) = k \times 180^o$) which is not within the normal operating region.

3.4 Existing Methodologies for Robust Nonlinear Excitation Control:

The DFL control law (3.16) can be applied to linearize the power system model equations (3.1 – 3.9) when all the necessary parameters are known. But when a large sudden fault occurs, or any network switching takes place, transmission line reactance x_L changes a lot which usually can not be measured or known. Such changes produces uncertainties in the power system model. It is to be noted that the uncertainty in x_L makes parameters x'_{ds}, x_{ds} and T'_d uncertain.

In [41-44] uncertainty in x_L has been treated by robust control theory [33-35] for linear system where the effect of uncertainty is modeled as parametric uncertainty in the linearized power system model equations (3.10 - 3.12) in the following way:

Choosing the state as $\mathbf{x}^T(t) = [\Delta\delta(t), \Delta\omega(t), \Delta P_e(t)]$, the power system model with parametric uncertainty becomes

$$\dot{\mathbf{x}}(t) = (\mathbf{A} + \Delta\mathbf{A})\mathbf{x}(t) + (\mathbf{B} + \Delta\mathbf{B})v_f(t) \tag{3.17}$$

Where

$$\mathbf{A} = \begin{bmatrix} 0 & 1 & 0 \\ 0 & -\frac{D}{2H} & -\frac{\omega_o}{2H} \\ 0 & 0 & -\frac{1}{T'_d} \end{bmatrix}; \quad \Delta\mathbf{A} = \begin{bmatrix} 0 & 0 & 0 \\ 0 & 0 & 0 \\ 0 & \beta & -\mu(t) \end{bmatrix}$$

$$\mathbf{B} = \left[0,\ 0,\ \frac{1}{T'_d}\right]^T ; \Delta\mathbf{B} = \left[0,\ 0,\quad \mu(t)\right]^T$$

Where $\Delta\mathbf{A}$ and $\Delta\mathbf{B}$ are parametric uncertainties, and

$$\mu(t) = \frac{1}{T'_d} - \frac{1}{T'_d + \Delta T'_d}$$

$$\Delta T'_d = \frac{x'_{ds} + \Delta x_L}{x_{ds} + \Delta x_L} T'_d; \qquad \Delta x_L \text{denote the ucertainty in } x_L$$

$$\overline{T}'_d = \frac{V_s^2}{x_{ds}} T'_d$$

$$\beta = \left[\frac{1}{T'_d} + \mu(t)\right]\left[\Delta\overline{T}'_d + \Delta T'_d Q_e(t)\right]$$

$$v_f(t) = k_e I_q(t) u_f(t) + T'_{do}(x_d - x'_d) I_q^2(t)\Delta\omega(t) + T'_d Q_e(t)\Delta\omega(t) + \overline{T}'_d \Delta\omega(t) - P_m$$

To solve the robust control problem for the linearized power system model (equation 3.17) following algebraic Riccati equation is required to be solved [42]:

$$\left(\mathbf{A} - \mathbf{B}\mathbf{R}^{-1}\mathbf{E}_2^T\mathbf{E}_1\right)^T \mathbf{P} + \mathbf{P}\left(\mathbf{A} - \mathbf{B}\mathbf{R}^{-1}\mathbf{E}_2^T\mathbf{E}_1\right) + \mathbf{P}\left(\alpha^2\,\mathbf{D}\mathbf{D}^T - \mathbf{B}\mathbf{R}^{-1}\mathbf{B}^T\right)\mathbf{P} + \mathbf{E}_1^T\left(\mathrm{I} - \mathbf{E}_2\mathbf{R}^{-1}\mathbf{E}_2^T\right)\mathbf{E}_1 = 0$$

where $\mathbf{R} = \mathbf{E}_2^T\mathbf{E}_2 > 0$, and

$$[\Delta\mathbf{A},\ \Delta\mathbf{B}] = \mathbf{D}\mathbf{F}(t)\,[\mathbf{E}_1,\ \mathbf{E}_2]$$

D, $\mathbf{E}_1$ and $\mathbf{E}_2$ are constant matrices;

$$\mathbf{D} = [0, \quad 0, \quad 1]^T ; \ \mathbf{E}_1 = \begin{bmatrix} 1, & 0 & 0 \\ 0 & \dfrac{|\beta|}{\gamma} & 0 \\ 0 & 0 & 1 \end{bmatrix}$$

$$\mathbf{E}_2 = [0, \quad 0, \quad 1]^T ; \ \mathbf{F}(t) = \left[0, \quad \gamma \frac{\beta}{|\beta|}, \quad -\mu(t) \right]$$

and $\mathbf{F}^T(t)\ \mathbf{F}(t) \le \alpha^2 \mathbf{I} \quad (\alpha > 0)$,

γ **i**s a constant.

Provided there exists a stabilizing solution $\mathbf{P} \geq 0$ for the Riccati equation, the robust linear control law is given by

$$\begin{aligned} v_f(t) &= -\mathbf{R}^{-1} \left(\mathbf{B}^T \mathbf{P} + \mathbf{E}_2^T \mathbf{E}_1 \right) \mathbf{x}(t) \\ &= -k_\delta \Delta\delta(t) - k_\omega \Delta\omega(t) - k_p \Delta P_e(t) \end{aligned}$$

and the DFL nonlinear control law is

$$u_f(t) = \frac{1}{k_e I_q(t)} \left[v_f(t) - T'_d Q_e(t) \Delta\omega(t) - \bar{T}'_d \Delta\omega(t) - (x_d - x'_d) T'_{do} \Delta\omega(t) I_q^2(t) + P_m \right] \quad (3.18)$$

Theoretically the method is very sound but difficulties may be encountered at the time of practical implementation. Determination of the bounds of parametrics uncertainties $\Delta\mathbf{A}$ $\Delta\mathbf{B}$ involves the determination of bounds on $\mu(t)$ $\Delta T'_d$ $\Delta \breve{T}'_d$ and β which may not be a trivial task for a real power system.

3.5 The Proposed DFL Control Strategy:

Comparing equations (3.5) and (3.6) the following is obtained:

$$P_e(t) = E_q(t)\, I_q(t) \qquad (3.19)$$

Applying the well known relation

$$E_q(t) = E'_q(t) + (x_d - x'_d)\, I_d(t)$$

and using equation (3.19):

$$P_e(t) = E'_q(t) I_q(t) + (x_d - x'_d) I_d(t) I_q(t)$$

Hence, $$\dot{P}_e(t) = \dot{E}'_q(t) I_q(t) + E'_q(t) \dot{I}_q(t) + (x_d - x'_d)\left(\dot{I}_d(t) I_q(t) + I_d(t) \dot{I}_q(t)\right)$$

$$= \frac{1}{T'_{do}}\left(E_f(t) - E_q(t)\right) I_q(t) + \left[E'_q(t) + (x_d - x'_d) I_d(t)\right] \dot{I}_q(t) + (x_d - x'_d) \dot{I}_d(t) I_q(t)$$

$$= \frac{1}{T'_{do}}\left[k_e u_f(t) I_q(t) - P_e(t)\right] + E_q(t) \dot{I}_q(t) + (x_d - x'_d) \dot{I}_d(t) I_q(t)$$

$$\Delta\dot{P}_e(t) = \frac{1}{T'_{do}}\left[k_e u_f(t) I_q(t) - \Delta P_e(t)\right] + E_q(t) \dot{I}_q(t) + (x_d - x'_d) \dot{I}_d(t) I_q(t) - \frac{1}{T'_{do}} P_m$$

$$= -\frac{1}{T'_{do}} \Delta P_e(t) + \frac{1}{T'_{do}} \hat{v}_f(t)$$

Where the new pseudo control law is given by

$$\hat{v}_f(t) = k_e u_f(t) I_q(t) + T'_{do}\left[E_q(t) \dot{I}_q(t) + (x_d - x'_d) \dot{I}_d(t) I_q(t)\right] - P_m \qquad (3.20)$$

and the DFL control law is given by

$$u_f(t) = \frac{1}{k_e I_q(t)}\left[\hat{v}_f(t) - T'_{do}\left(E_q(t)\dot{I}_q(t) + (x_d - x'_d)\dot{I}_d(t)I_q(t)\right) + P_m\right] \qquad (3.21)$$

The linearized model has the following form:

$$\Delta\dot{\delta}(t) = \Delta\omega(t) \qquad (3.22)$$

$$\Delta\dot{\omega}(t) = -\frac{D}{2H}\Delta\omega(t) - \frac{\omega_o}{2H}\Delta P_e(t) \qquad (3.23)$$

$$\Delta\dot{P}_e(t) = -\frac{1}{T'_{do}}\Delta P_e(t) + \frac{1}{T'_{do}}\hat{v}_f(t) \qquad (3.24)$$

It is to be noted that the proposed DFL control law (3.21) is locally realizable at the generator terminals. T'_{do} and x_{ad} are obtained from manufacturer's specifications or can be measured from standard tests [53-56]. $P_e(t)$ and $I_f(t)$ are measurable at the machine terminals, and, hence, $I_q(t)$ and $E_q(t)$ can be computed from equations (3.6) and (3.8) respectively. $\dot{I}_d(t)$ and $\dot{I}_q(t)$ can also be derived at the generator terminals.

In the present study the two derivatives $\dot{I}_d(t)$ and $\dot{I}_q(t)$ are calculated by a simple backward difference formula from two successive samples in the following way:

$$\dot{I}_d(t_{k+1}) = \frac{I_d(t_{k+1}) - I_d(t_k)}{\Delta T}$$

and

$$\dot{I}_q(t_{k+1}) = \frac{I_q(t_{k+1}) - I_q(t_k)}{\Delta T}$$

Where, t_k and t_{k+1} are two successive sampling instants and $\Delta T = (t_{k+1} - t_k)$ is the sampling interval.

It may be noted that the values of $\dot{I}_d(t)$ and $\dot{I}_q(t)$ calculated after the first sample following any network switching operation may assume very large figure and should be discarded as grossly erroneous data. In that case, as has been done in the present simulation, the values of $\dot{I}_d(t)$ and $\dot{I}_q(t)$ calculated and stored last before the switching operation takes place, can be used as an approximation of the current values of $\dot{I}_d(t)$ and $\dot{I}_q(t)$. However, in real-world application, median filtering technique [61] can be a very good alternative for obtaining a reliable differentiator.

An inspection of the power system model (equations 3.10 – 3.12) and the control law (equation 3.14) reveals that the uncertain terms are T'_d and x_{ds}. They result from external disturbances such as changes in x_L which can not be measured locally. As a result, uncertainties appear both in the model parameter (T'_d in this case) and the input $v_f(t)$, which necessitates the application of robust control technique that is difficult from the point of view of practical implementation. In the contrary, the proposed DFL control law (equations 3.20 and 3.21) transforms the nonlinear power system model (equations 3.1 – 3.3) into a linearized one (equations 3.22 – 3.24) which is free from any parametric uncertainties. The generator parameters D,H and T'_{do} are independent of system operating conditions and network configurations. Therefore, it is not unreasonable to assume that their values are known with sufficient degree of certainty. It is, therefore, quite appropriate to say that the expression (equatic $\hat{v}_f(t)$ for incorporates all the effects of uncertainties (see Appendix – I) arising from external disturbances in terms of measurable or computible quantities. Consequently, the new DFL control law possesses disturbance rejection property, and hence, it is a robust control law.

$\hat{v}_f(t)$ can be determined by any linear system control method [36,37]. In this work, LQ optimal control method has been applied for the determination of $\hat{v}_f(t)$ which gives the following linear state feedback law:

$$\hat{v}_f(t) = -\hat{k}_\delta \Delta\delta(t) - \hat{k}_\omega \Delta\omega(t) - \hat{k}_p \Delta P_e(t)$$

Implementation of the above feedback law requires that the desired post-fault equilibrium values of the states be known. While ω_o and P_m are known, the desired post-fault equilibrium δ_o is usually not known or can not be determined without a full scale load flow study. This difficulty can be overcome by applying the observation decoupled state space [62]. Here, for the simple case of SMIB system, the value of post-fault δ_o has been assumed to be known.

In the following sections results of simulation are shown and discussed to demonstrate the efficacy of the proposed control strategy.

3.6 The Study System:

Fig. 3.1 shows the SMIB power system that has been used in the present work.

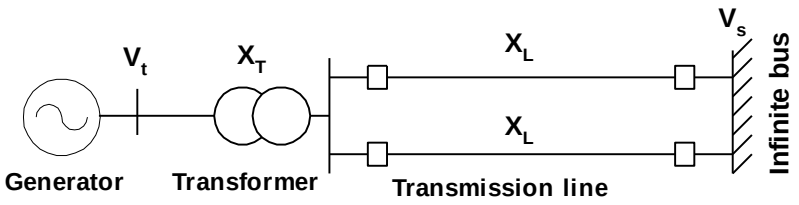

Fig.3.1: SMIB power system model

The necessary system data used in the simulation studies are available in [39, 42] and are also produced below for ready reference:

$\omega_o = 314.159$; $D = 5.0$; $H = 8.0$ secs.

$T'_{do} = 6.9$ secs ; $k_e = 1$

$x_d = 1.863$; $x'_d = 0.257$; $x_{ad} = 1.712$

$x_T = 0.127$; $x_L = 0.4853$

The physical limit of the excitation voltage is

max $E_f(t) = 7.0$ p.u.

min $E_f(t) = -6.4$ p.u.

The prefault operating point is

(i) $\delta_o = 72^o$; $P_m = 0.9$ p.u. ; $V_{to} = 1.0$ p.u.

(ii) $\delta_o = 47^o$; $P_m = 0.45$ p.u. ; $V_{to} = 1.003$ p.u.

The following fault sequences have been considered:

Fault sequence 1 : ***Permanent fault:***

Stage 1: The system is in a prefault steady state;

Stage 2: A fault occurs at $t = t_o$

Stage 3: The fault is removed by opening the breakers of the faulted line at $t = t_1$;

Stage 4: The system is in a post-fault state.

Fault sequence 2: ***Temporary fault:***

Stage 1: The system is in a prefault steady state

Stage 2: A fault occurs at $t = t_o$;

Stage 3: The fault is removed by opening the breakers of the faulted line at $t = t_1$;

Stage 4: The transmission line are restored with the fault cleared at $t = t_2$;

Stage 5: The system is in a post fault state.

The fault considered is a symmetrical 3-phase short circuit fault which occurs on one of the transmission lines. The fault location is indexed by a positive number λ which is the fraction of the faulted line to the left of the fault. $\lambda = 0$ indicates the H.T. terminal of the transformer, $\lambda = 0.5$ indicates the midpoint of the line and so on.

LQ optimal control solution generates the following values for the gain co-efficients:

$\hat{K}_{\delta} = 22.3607$; $\hat{K}_{\omega} = 7.8317$; $\hat{K}_{p} = 55.4999$

Hence, $\ddot{U}_f(t)$ used in the simulation is given by

$$\hat{v}_f(t) = 22.3607\ \Delta\delta(t) + 7.8317\ \Delta\omega(t) - 55.4999\ \Delta P(t)$$

The next section shows the simulation results.

3.7 Simulation Results:

This section shows the simulation results to demonstrate the effectiveness of the proposed excitation control strategy. Operating condition (i) and fault sequence – I have been considered first. The time of fault occurrence, t_o = 0.1 secs. has been assumed in all cases. Fig.3.2 (a) shows the power angle response for λ = 0.05 and with no excitation control (i.e. $E_f(t)$ remains constant at its pre-fault value). It is seen that with no excitation control the system becomes unstable for a fault clearing time, t_1 = 0.21 secs. While it is just stable for t_1 = 0.20 secs. The post-fault response is, however, highly oscillatory which is undesirable.

From Fig.3.2(b) it can be seen that with the application of the proposed excitation control, the critical fault clearing time for the above fault increases upto 0.27 secs. and, moreover, the post-fault response is also fairly damped. With the fault cleared at t_1 = 0.28 secs. the power angle response is, however, unstable even with the excitation control.

Fig.3.2(c) demonstrates the effect of the proposed control for different fault locations with same fault clearing time, t_1 = 0.27 secs. Every-time smooth and quick transition to a post-fault steady state is achieved without much undesirable oscillations.

The effect of different fault clearing time is demonstrated in Fig.3.2 (d) which shows the power angle responses for λ = 0.25 with t_1 = 0.30 secs. and λ = 0.5 with t_1 = 0.35 secs. As is clear from the figure, in both cases very good stable responses are obtained.

Fig. 3.2(e) demonstrates the effect of the proposed control for fault sequence – II. Results are shown for λ = 0.05 and λ = 0.25. For both cases t_1 and t_2 are 0.27 secs and 1.0 secs. respectively. Very good transient response and rapid convergence to post-fault steady state are obtained in both cases.

Fig.3.3(a) – 3.3(d) display the same for operating point (ii). The different cases considered are same as those done for operating point (i). The figures are self explanatory and from these figures it is clear that the proposed excitation control is equally effective for pre-fault operating point (ii) also.

So, the simulation results amply demonstrates that the proposed DFL excitation control is very effective in enhancing transient stability and achieving very good post-fault, fault location and post-fault network conditions.

Fig.3.2(a): Power angle response with no excitation control

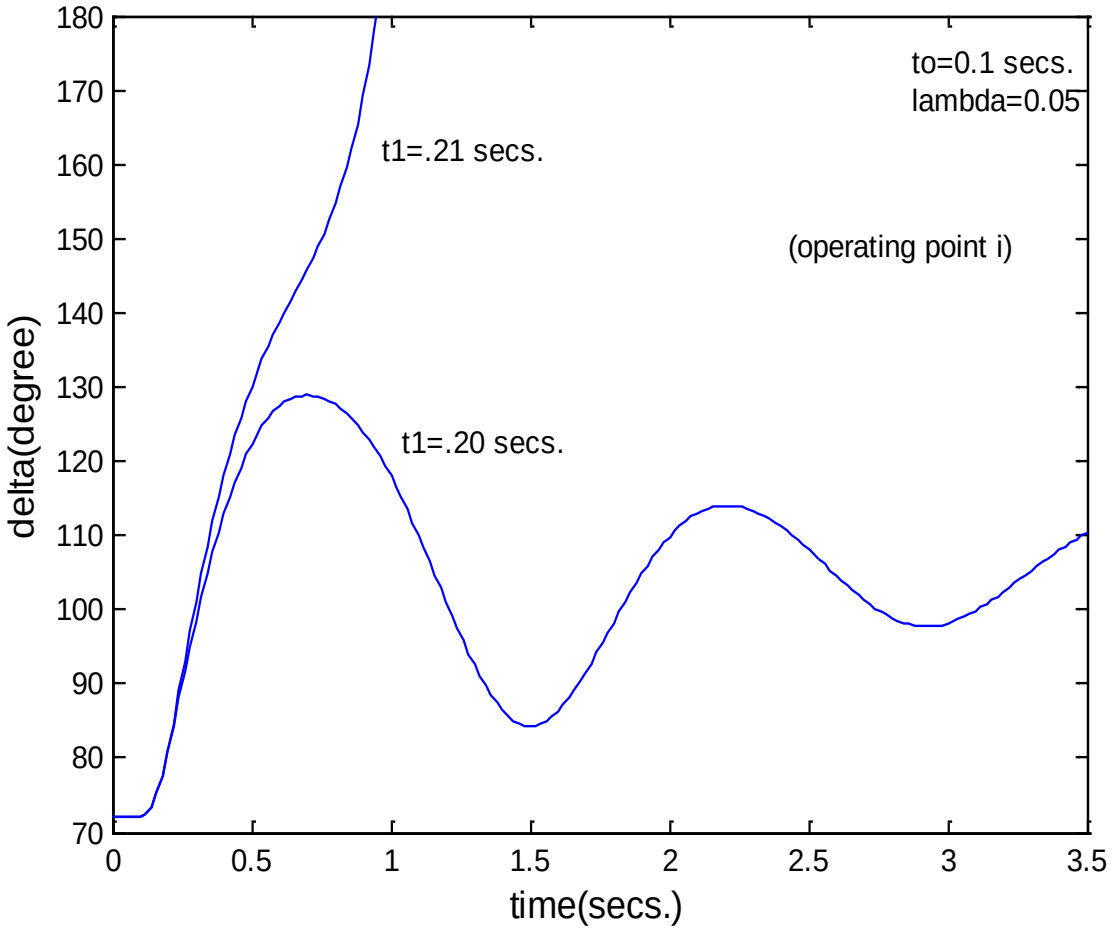

Fig.3.2(b): Power angle response with proposed excitation contrl

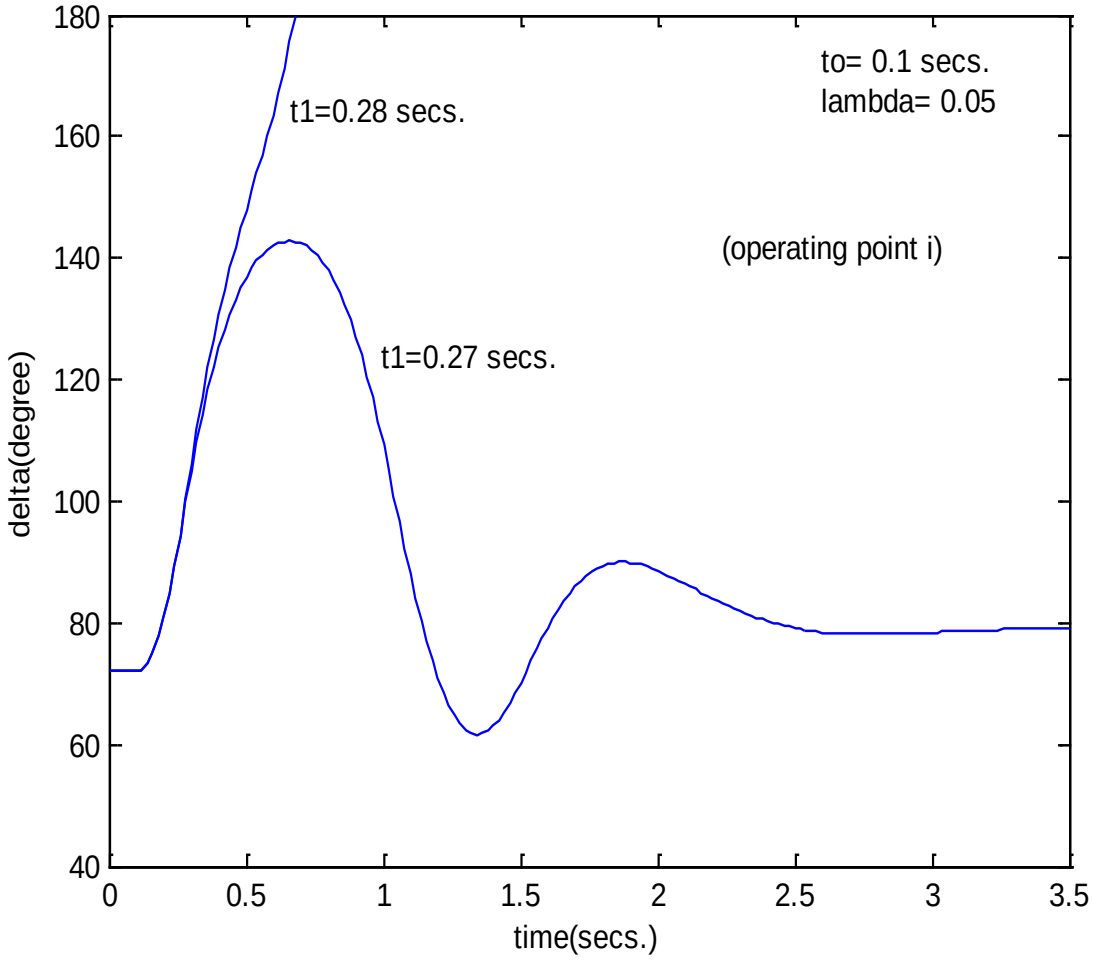

Fig.3.2(c): Power angle response for different lambda

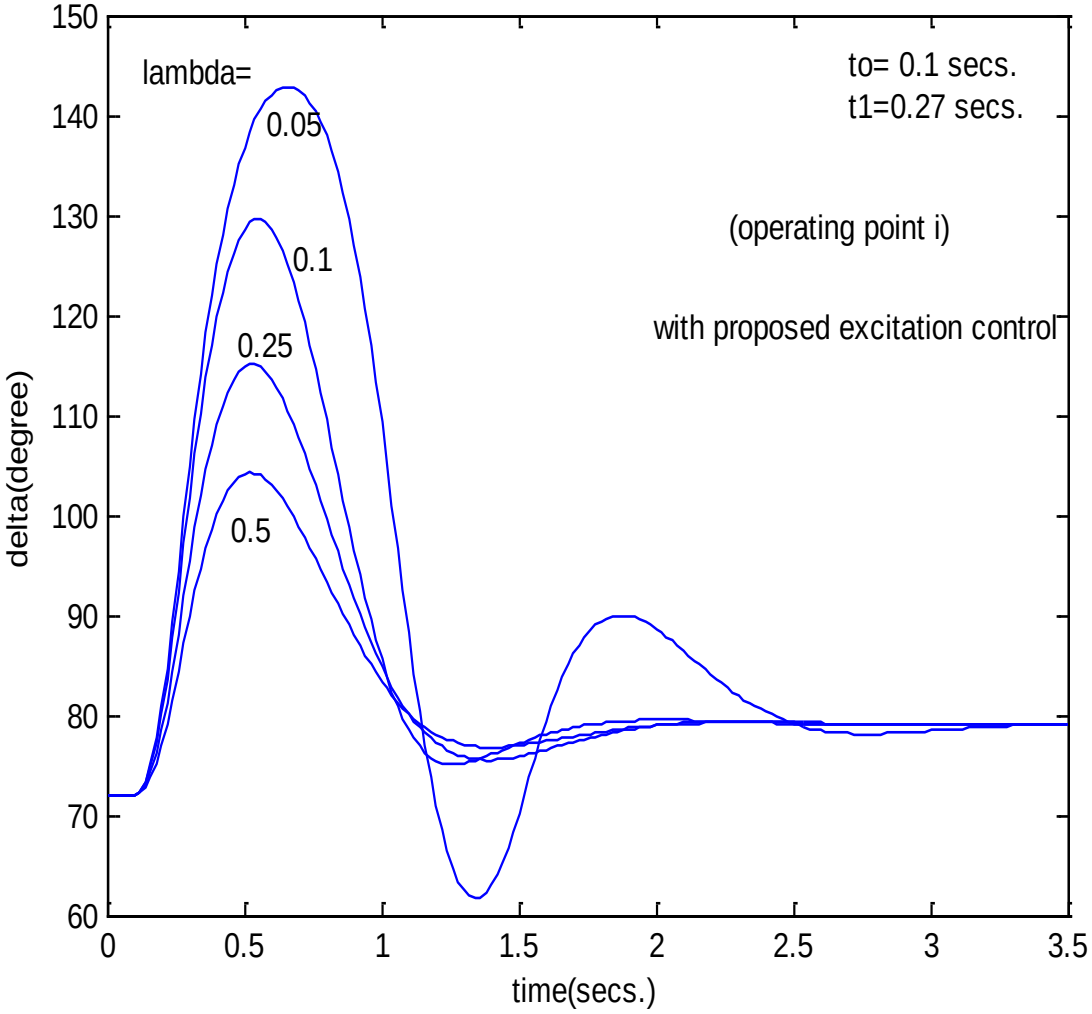

Fig.3.2(d): Power angle response for different fault clearing time

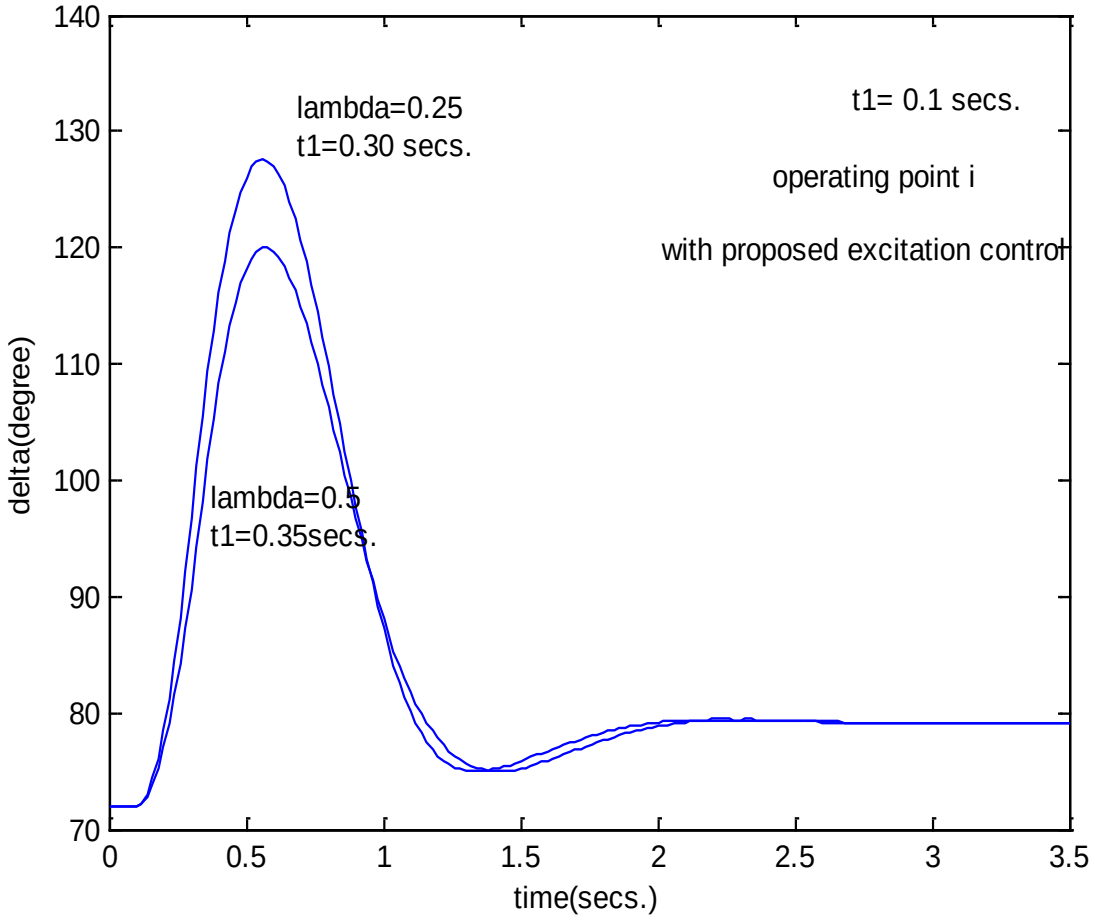

Fig.3.2(e): Power angle response for temporary fault

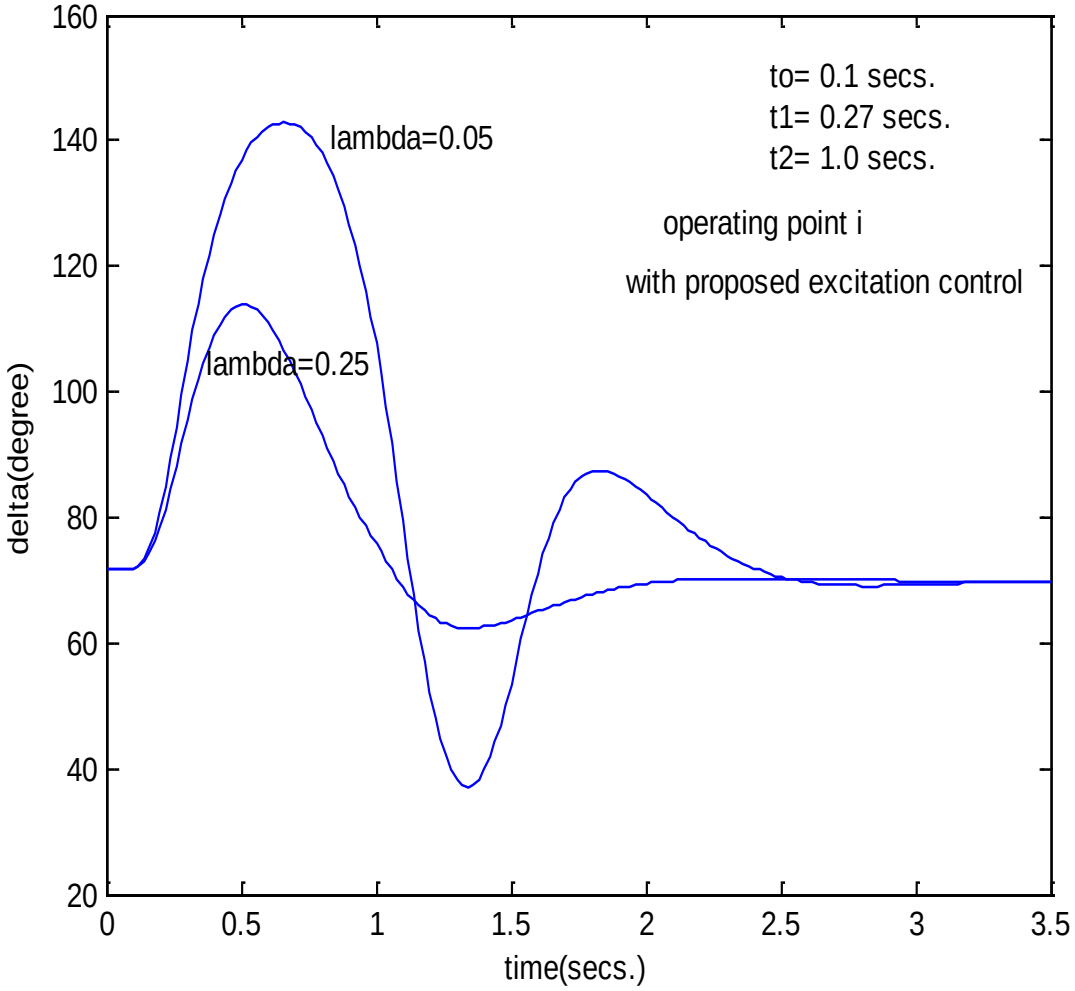

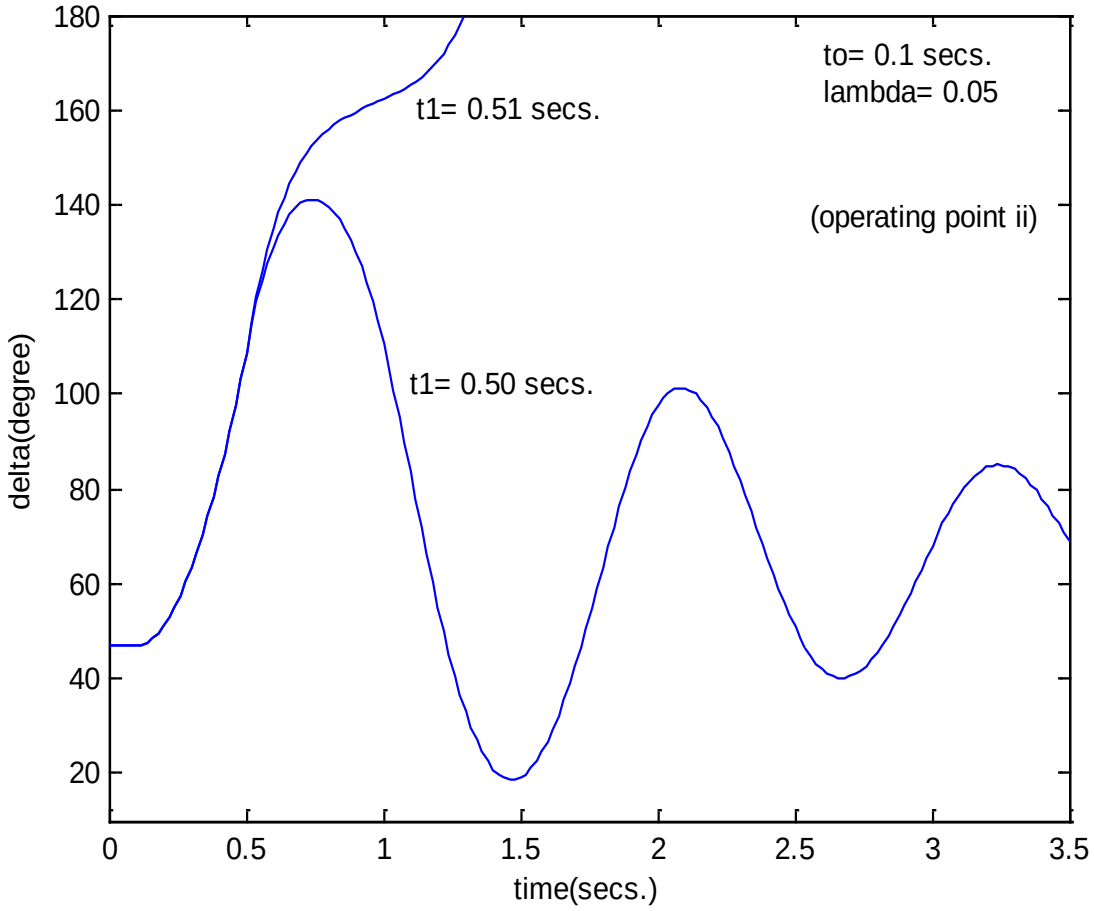
180
160
140
120
100
80
60
40
20
0
0.5
1
1.5
2
2.5
3
3.5
delta(degree)
time(secs.)
to= 0.1 secs.
lambda= 0.05
t1= 0.51 secs.
(operating point ii)
t1= 0.50 secs.

Fig.3.3(b): Power angle response with proposed control

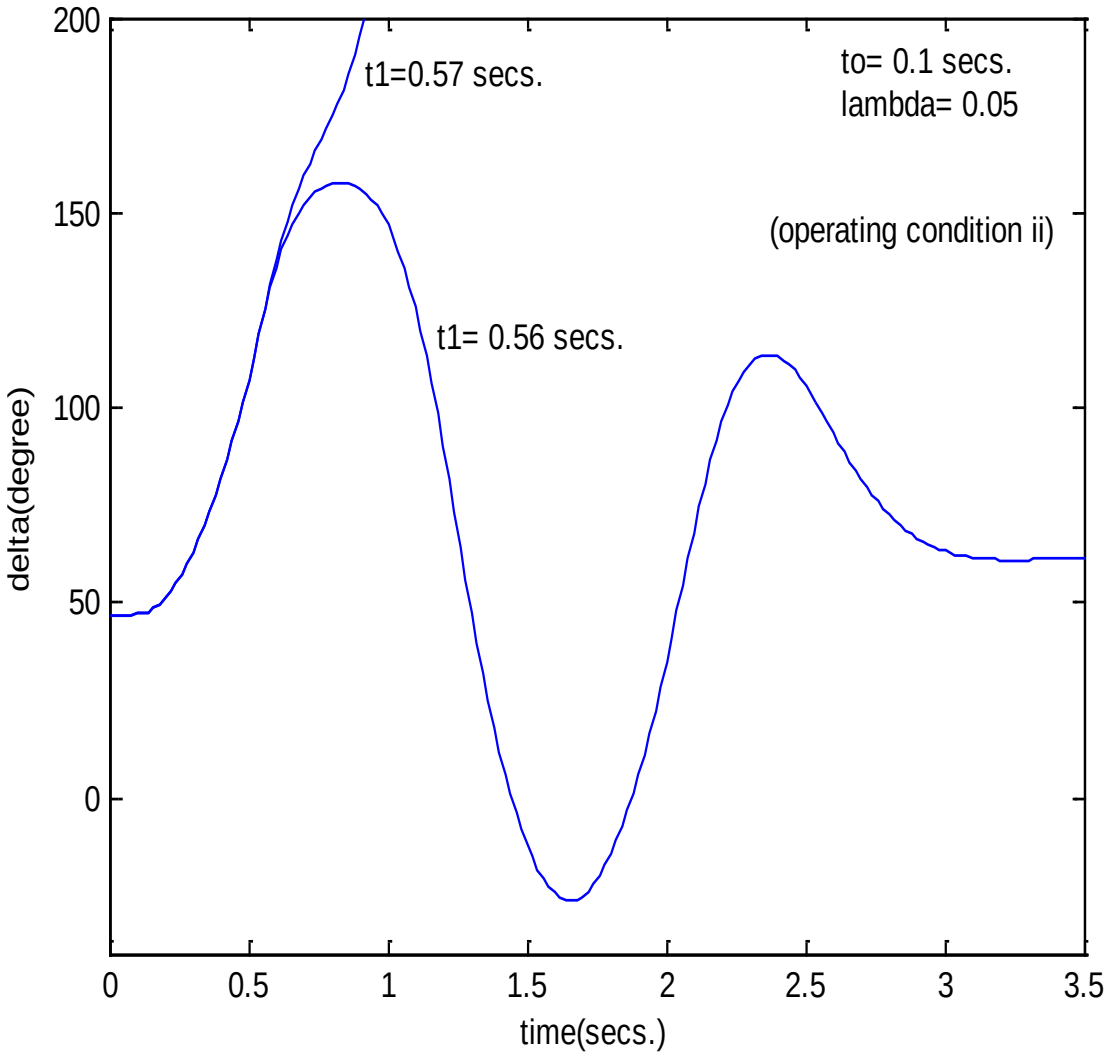

Fig.3.3(c): Power angle response for different fault locations

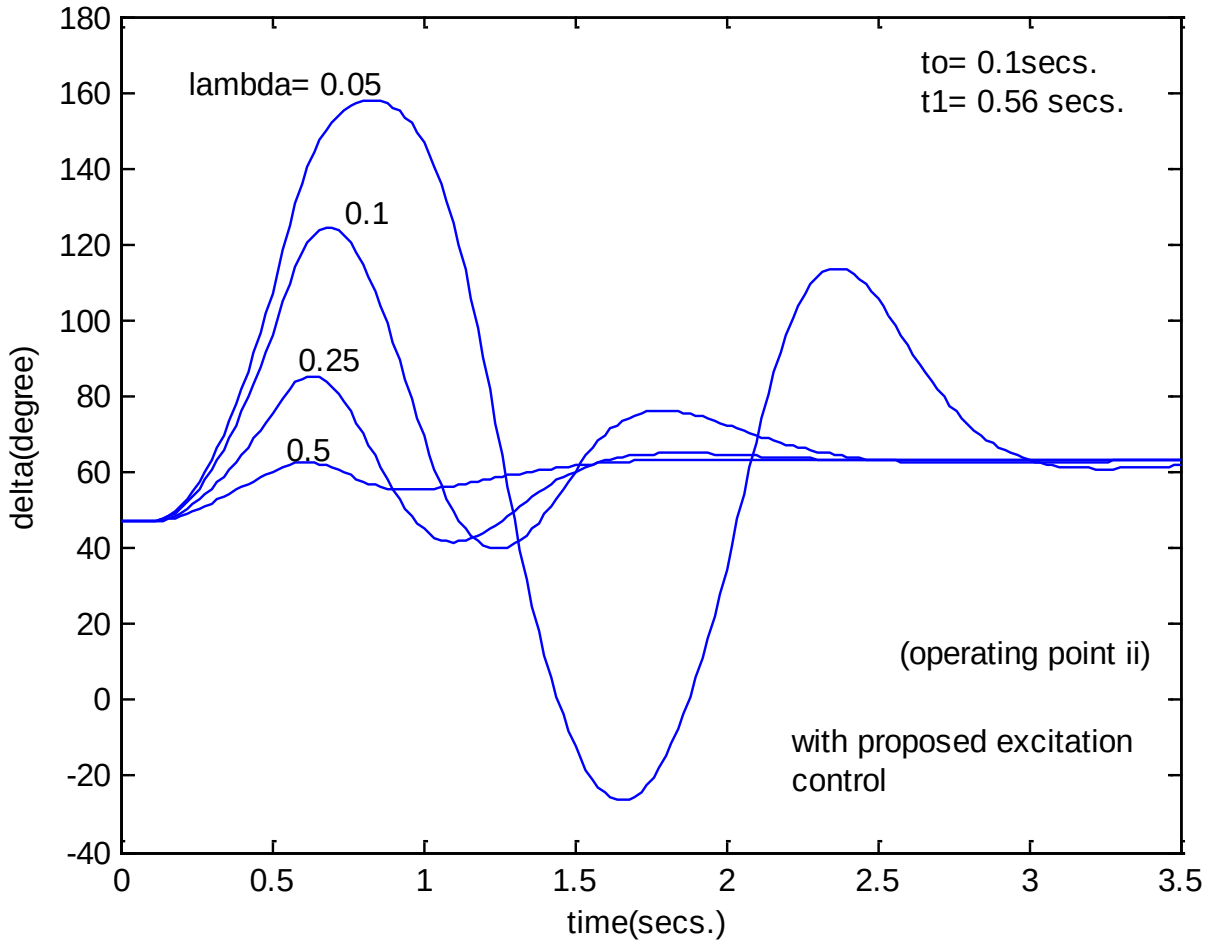

Fig.3.3(d) Power angle response for different fault clearing times

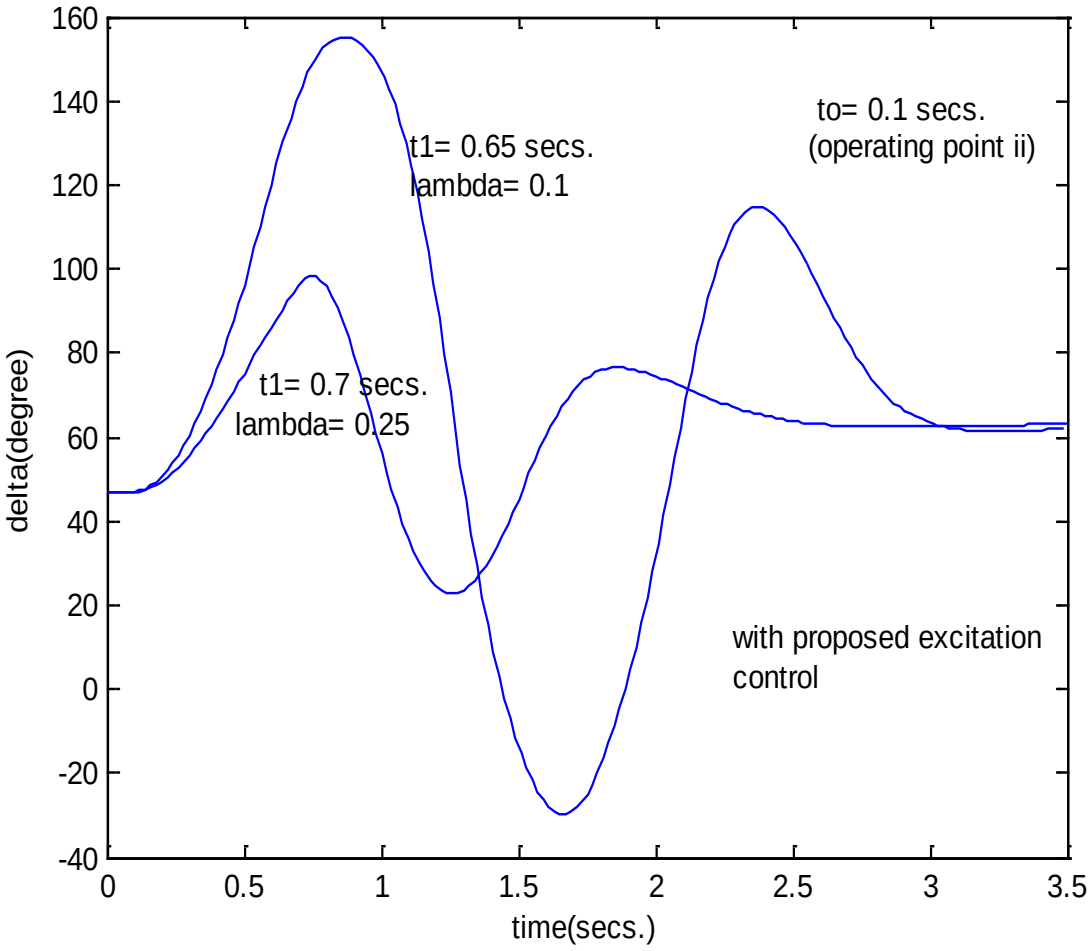

Fig.3.2(c): Power angle response for different lambda with proposed excitation control

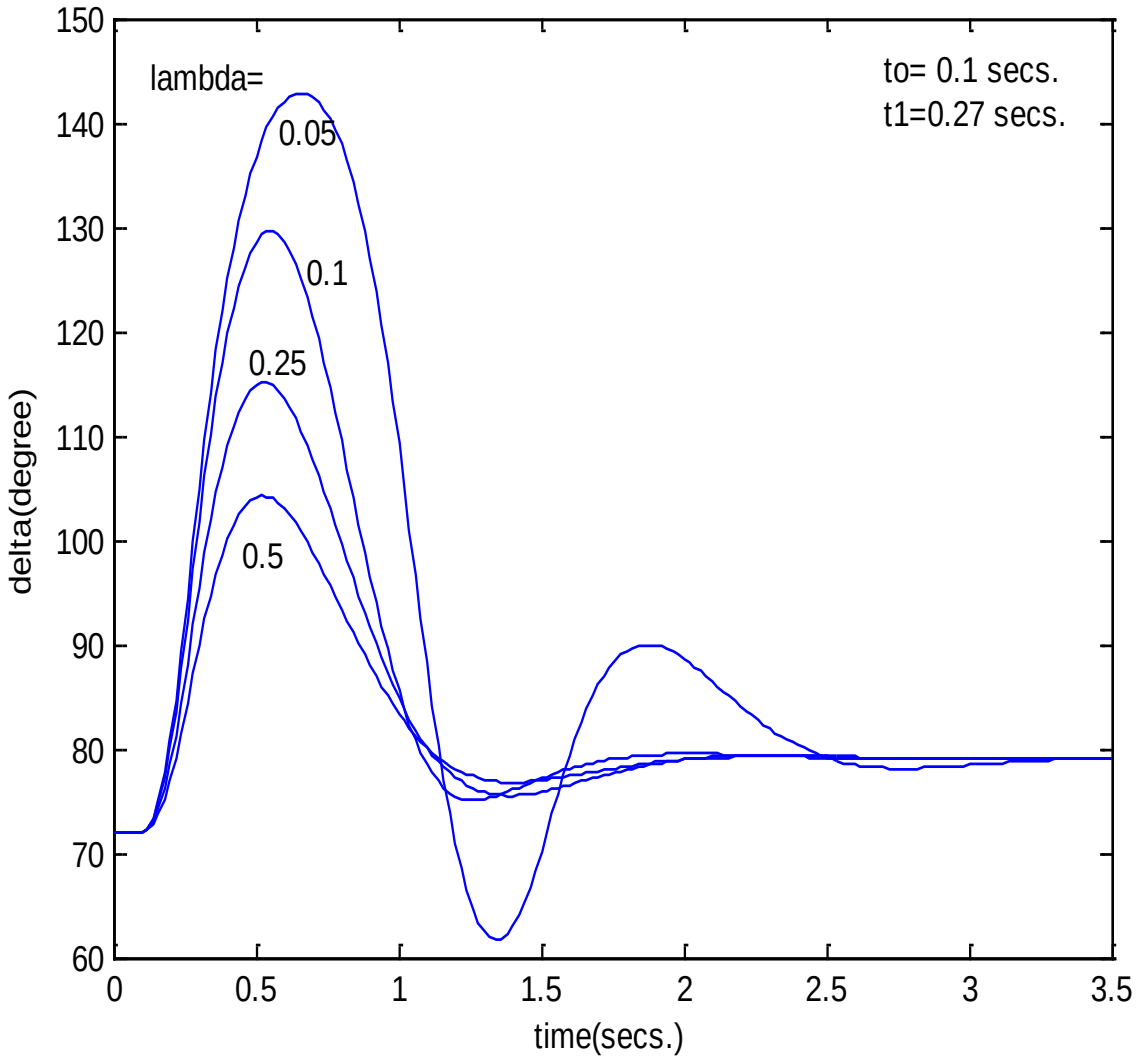

Fig.3.2(d): Power angle response for different fault clearing time